

EVAPORATION AND CONDENSATION OF H I CLOUDS IN THERMALLY BISTABLE INTERSTELLAR MEDIA:
SEMI-ANALYTIC DESCRIPTION OF ISOBARIC DYNAMICS OF CURVED INTERFACESMASAHIRO NAGASHIMA,¹ HIROSHI KOYAMA,² AND SHU-ICHIRO INUTSUKA¹*Draft version February 7, 2020*

ABSTRACT

We analyze the evaporation and condensation of spherical and cylindrical H I clouds of the cold neutral medium surrounded by the warm neutral medium. Because the interstellar medium including those two phases is well described as a thermally bistable fluid, it is useful to apply pattern formation theories to the dynamics of the interface between the two phases. Assuming isobaric evolution of fluids and a simple cubic form of the heat-loss function, we show the curvature effects of the interface. We find that approximate solutions for spherical clouds are in good agreement with numerically obtained solutions. We extend our analysis to general curved fronts taking into account the curvature effects explicitly. We find that the curvature effects always stabilize curved fronts.

Subject headings: hydrodynamics – ISM: clouds – ISM: kinematics and dynamics – methods: analytical

1. INTRODUCTION

It is widely known that the interstellar medium (ISM) is well described as a thermally bistable fluid owing to radiative cooling and heating due to external radiation fields and cosmic rays (Field, Goldsmith & Habing 1969; Wolfire et al. 2003). Two stable phases are called the warm neutral medium (WNM) with temperature $T \sim 10^4$ K and the cold neutral medium (CNM) with $T \sim 10^{1-2}$ K, respectively. Gas in an unstable phase with temperature between the WNM and CNM is decomposed into the two stable phases via thermal instability (Field 1965; Balbus 1986). These stable phases can be connected through interfaces in pressure equilibrium. It is important for understanding the behavior of the ISM such as the interstellar turbulence (Koyama & Inutsuka 2002, 2004; Kritsuk & Norman 2002a,b) and the evolution of galaxies (e.g. McKee & Ostriker 1977) to clarify the dynamics of the interface or *front*, which corresponds to the evaporation and condensation of low temperature H I clouds.

Zel'dovich & Pikel'ner (1969) and Penston & Brown (1970) considered isobaric and steady phase-change in the bistable fluid assuming plane-parallel geometry. In this case, because the mass flux across the interface conserves, the velocity of fluids can be estimated as an eigenvalue of the energy equation. Then they pointed out the relationship between the motion of fronts, which determines the rate of evaporation or condensation of clouds, and external pressure, and the existence of *saturation* pressure at which a static front can exist. After that, many authors have investigated the thermally bistable flow (e.g. Ferrara & Shchekinov 1993; Hennebelle & Pérault 1999). Elphick, Regev & Spiegel (1991) and Elphick, Regev & Shaviv (1992, hereafter ERS92) treated with fluid equations in a more sophisticated manner in plane-parallel geometry. In the latter work, they formulated equations in the Lagrangian coordinate. Combined with the isobaric assumption, they derived a second-order ordinary differential equation in a steady state from the energy equation. Moreover, they discussed the

behavior of steady solutions from a pattern-theoretical point of view.

It is challenging to extend those analyses to higher dimensions while it is much useful for applying to realistic situations. Graham & Langer (1973) numerically computed isobaric flows in three dimensional spherical geometry for the first time. They pointed out the existence of a critical size of clouds to avoid evaporation. Based on ERS92, Shaviv & Regev (1994) argued the case of higher dimensions. However, it is difficult to extend the Lagrangian formulation in plane-parallel geometry provided by ERS92 to higher dimensional geometry in a straightforward manner. Therefore assuming a model equation similar to the Ginzburg-Landau (GL) equation, they derived the speed of frontal motion. Surprisingly, they have showed that the dependence of the frontal speed on time, or radii of clouds, is dependent on the dimension of geometry. Besides they have claimed that their conclusion is supported by numerical simulations. It should be noted that Aranson, Meerson & Sasorov (1995) also discussed the front curvature effects in a confined plasma, in which the boundary conditions are different from ours. Thereby their methods are inapplicable to the ISM in a straight forward way.

Thus, the purpose of this paper is to reanalyze the frontal motion in d -dimensional spherically symmetric geometry, aided by pattern formation theories (e.g. Bray 1994). This paper is outlined as follows. In §2 we briefly review ERS92 to prepare the analysis in higher dimensional geometry. In §3 we show a systematic procedure to derive the curvature effects. In §4 we discuss the dynamics of general curved fronts. In §5 we provide conclusions and discussion.

2. LAGRANGIAN DESCRIPTION IN PLANE-PARALLEL GEOMETRY

In the following, we assume isobaric evolution in which pressure is uniform over the whole system because the fluid motion is much slower than the sound speed. The basic fluid equations under the assumption of isobaric evolution are written as

$$\frac{\partial \rho}{\partial t} + \nabla \cdot \rho \mathbf{v} = 0, \quad (1)$$

$$\frac{\gamma}{\gamma-1} \frac{\mathcal{R}}{\mu} \rho \frac{dT}{dt} + \rho \mathcal{L} - \nabla \cdot \kappa(T) \nabla T = 0, \quad (2)$$

$$p = \rho \frac{\mathcal{R}}{\mu} T, \quad (3)$$

Electronic address: masa@scphys.kyoto-u.ac.jp

¹ Department of Physics, Graduate School of Science, Kyoto University, Sakyo-ku, Kyoto 606-8588, Japan² Department of Earth and Planetary Science, Kobe University, Kobe 657-8501, Japan

where the equation of motion is omitted because of the isobaric assumption, $\kappa(T)$ is the conductivity, \mathcal{R} the gas constant, μ the mean molecular weight, and γ the adiabatic index. The heat-loss function, \mathcal{L} , is defined as $\rho\Lambda - \Gamma$, where Λ and Γ are the cooling and heating rates, respectively. Throughout this paper, we assume a single power-law of the conductivity, $\kappa(T) = \kappa_0(T/T_0)^\alpha$, and $\alpha = 1/2$ for neutral gas. Dividing variables by characteristic values, we obtain dimensionless quantities, $\tilde{T} = T/T_0$, $\tilde{\rho} = \rho/\rho_0$, and $\tilde{p} = p/p_0$, and introducing characteristic length l_F and time-scale t_0 , we obtain $\tilde{\mathbf{v}} = \mathbf{v}/(l_F/t_0)$. Here we take t_0 as the cooling time-scale,

$$t_0 = \frac{\gamma}{\gamma - 1} \frac{\mathcal{R}T_0}{\mu\rho_0\Lambda_0}, \quad (4)$$

where Λ_0 is the cooling rate at the characteristic temperature, T_0 , and l_F as the Field length (Field 1965),

$$l_F = \sqrt{\frac{\kappa_0 T_0}{\rho_0^2 \Lambda_0}}. \quad (5)$$

Using these quantities, the basic equations become the following dimensionless form,

$$\frac{\partial \tilde{\rho}}{\partial \tau} + \nabla \cdot \tilde{\rho} \tilde{\mathbf{v}} = 0, \quad (6)$$

$$\frac{d\tilde{T}}{d\tau} + \tilde{\mathcal{L}} - \frac{1}{\tilde{\rho}} \nabla \cdot \tilde{T}^\alpha \nabla \tilde{T} = 0, \quad (7)$$

$$\tilde{p} = \tilde{\rho} \tilde{T}, \quad (8)$$

where $\tau = t/t_0$ and $\tilde{\mathcal{L}} = \mathcal{L}/\rho_0\Lambda_0$.

It is useful to transform these equations into the Lagrangian description particularly in one dimensional case as shown in ERS92. Using a relation $dm = \tilde{\rho}dx$, where x is the dimensionless Eulerian coordinate normalized by l_F and m is the Lagrangian coordinate, the energy equation (7) is converted as follows,

$$\partial_\tau \tilde{T} = -\tilde{\mathcal{L}} + \tilde{p} \partial_m \tilde{T}^{\alpha-1} \partial_m \tilde{T}, \quad (9)$$

where (τ, m) are the independent dimensionless variables and ∂_t and ∂_m denote $(\partial/\partial t)$ and $(\partial/\partial m)$, respectively. Further transformation introducing $Z = \tilde{T}^\alpha$ makes the above equation simpler,

$$\partial_\tau Z = F(Z) + \tilde{p} Z^\beta \partial_m^2 Z^2, \quad (10)$$

where $\beta = 1 - 1/\alpha$ and $F(Z) = -\alpha Z^\beta \tilde{\mathcal{L}}$. Note that this simple form is obtained only in the one dimensional case. ERS92 assumed a simple form of $F(Z)$, which mimics the real heat-loss function,

$$F(Z) = Z^\beta [\Delta^2(Z - Z_2) - (Z - Z_2)^3 - D \log \tilde{p}], \quad (11)$$

where D is a positive constant.

To obtain a traveling wave solution, we define $\chi = m - c_m \tau$, where c_m is a constant which is a velocity on the Lagrangian coordinate. Then the partial differential equation (10) becomes an ordinary differential equation,

$$\tilde{p} Z^\beta Z'' + c_m Z' + F(Z) = 0, \quad (12)$$

where the prime means differentiation with respect to χ .

An analytic kink solution connecting the two stable phases is obtained when $c_m = 0$ as shown in ERS92. The solution Z_0 is

$$Z_0(m) = Z_2 + \Delta \tanh \left[\frac{\Delta}{\sqrt{2}} (m - m_c) \right]. \quad (13)$$

Unfortunately, as mentioned above and as shown in Shaviv & Regev (1994), it is difficult to extend it to higher dimensional cases. This can be easily seen if we take a d -dimensional ($d \geq 2$) continuity, $dm \propto r^{d-1} dx$. Because this dependence on d produces a term explicitly depending on m , the second derivative ∂_m^2 cannot be regarded as ∇_m^2 . To avoid this difficulty, Shaviv & Regev (1994) assumed that a time-dependent GL (TDGL) equation (e.g. Bray 1994) in the Lagrangian space is a good approximation for the evolution of a spherical cloud. To be free from such an assumption, it is fruitful to be back in the Eulerian space to treat the fluid equations in higher dimensions.

3. HIGHER DIMENSIONAL CASES: SPHERICAL AND CYLINDRICAL GEOMETRY

In the Eulerian space (τ, r) , introducing $X = \tilde{T}^{1+\alpha}$, we obtain the continuity and energy equations,

$$\frac{dX}{d\tau} - (1 + \alpha) X \nabla \cdot \mathbf{v} = 0, \quad (14)$$

$$\frac{dX}{d\tau} = \frac{1 + \alpha}{\alpha} X^{1/(1+\alpha)} F[Z] + \frac{1}{\tilde{p}} X \nabla^2 X. \quad (15)$$

Transforming the coordinate to $\chi = r - R_d(\tau)$ for a d -dimensional spherical cloud,

$$-\dot{R}_d X' = -v X' + (1 + \alpha) X v' + (1 + \alpha) \frac{d-1}{r} v X \quad (16)$$

$$\begin{aligned} -\dot{R}_d X' = & -v X' + \frac{1 + \alpha}{\alpha} X^{1/(1+\alpha)} F[Z] \\ & + \frac{1}{\tilde{p}} X'' X + \frac{1}{\tilde{p}} \frac{d-1}{r} X' X, \end{aligned} \quad (17)$$

where $\dot{R}_d = dR_d/d\tau$ and F is given by eq.(11). The radius of the cloud, $R_d(\tau)$, is hereafter defined to be the position at $X = X_2 \equiv Z_2^{(1+\alpha)/\alpha}$. The fluid velocity v is defined in the rest frame of the center of the cloud. By defining $u_d \equiv v - \dot{R}_d$, which is the fluid velocity in the rest frame of the front, the above equations become

$$u_d X' = (1 + \alpha) X u'_d + (1 + \alpha) \frac{d-1}{r} (u_d + \dot{R}_d) X, \quad (18)$$

$$u_d X' = \frac{1 + \alpha}{\alpha} X^{1/(1+\alpha)} F[Z] + \frac{1}{\tilde{p}} X'' X + \frac{1}{\tilde{p}} \frac{d-1}{r} X' X. \quad (19)$$

Because we take $v = 0$ at the cloud center, u_d must be $-\dot{R}_d$ in the vicinity of the center. In the plane-parallel case $d = 1$, using the relationship $\tilde{T} = X^{1/(1+\alpha)} = Z^{1/\alpha}$ and $\tilde{\rho} u_d = -c_m$, eq.(17) can be reduced to eq.(7), and therefore the kink solution eq.(10) is easily proved to satisfy these equations when $\dot{R}_1 = 0$.

The above equations are non-linear, so it is hard to find an analytic solution. Therefore we simply assume what follows. One is that the structure of a solution is very similar to a one-dimensional ($d = 1$) solution. The second assumption is that the first derivative of the solution is sharply peaked at the interface, in other words, the width of the interface is very narrow compared to the scale of the cloud size. This corresponds to $X' = 0$ at $r \neq R_d$. Under these assumptions, it is reasonable to substitute the first and second terms of the right-hand side of eq.(19) into $u_1 X'$. Thus we obtain an approximate form,

$$u_d(R) = u_1(R) + \frac{1}{\tilde{p}} \frac{d-1}{R_d} X_2, \quad (20)$$

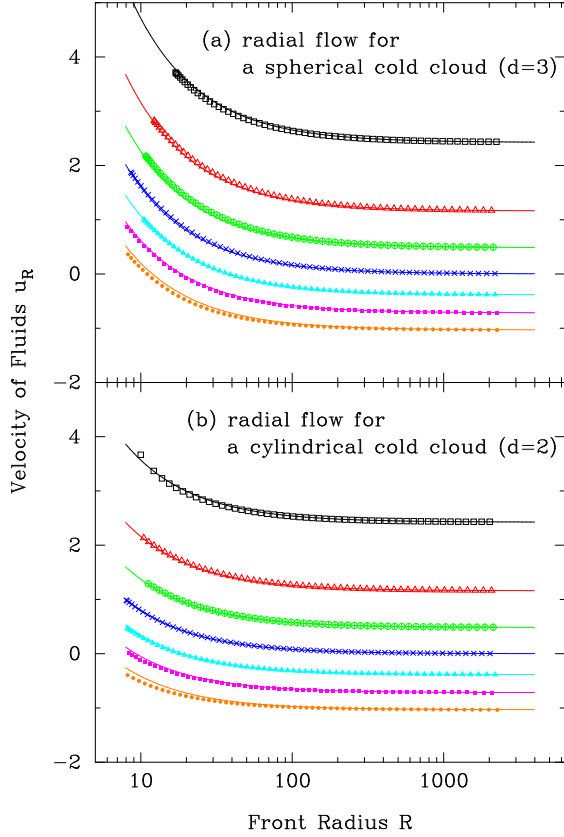


FIG. 1.— Fluid velocity $u_d(R)$ against radius R for (a) $d = 3$ (sphere) and (b) $d = 2$ (cylinder). The curves and symbols represent the approximate solution, eq.(20), and the numerical solution given by eqs.(16) and (17). From the top to the bottom, $\tilde{p} = 0.7, 0.8, 0.9, 1, 1.1, 1.2$ and 1.3 , respectively. We set $Z_2 = 2$ and $\Delta = D = 1$ for simplicity.

where $u_d(R)$ is the fluid velocity passing the front at $r = R_d$ in the front rest frame. X_2 in the last term emerges because we define the position of the front at which $X = X_2$. This is similar to an equation discussed by Graham & Langer (1973).

Fig.1 shows the fluid velocity at the front, $u_d(R_d)$, against R_d for $d = 2$ and 3 . The curves and symbols represent those given by the approximate solutions and numerical ones, respectively, for different values of pressure. Clearly the above approximate solution well agrees with the numerical solutions. In the large limit of R_d , we have confirmed that the fluid velocity converges on $u_1(R)$. Note that the cloud evaporates when u_d is positive, and vice versa.

To estimate the front velocity, we need to know the relationship between $u_d(R)$ and \dot{R}_d . Here we evaluate $f \equiv -\dot{R}_d/u_d(R)$ from the results for $d = 1$ case. Noting that c_m in eq.(13) corresponds to the mass flux, $c_m = -\tilde{\rho}u_1$, $u_1(R)$ can be written as

$$u_1(R) = -c_m X_2^{1/(1+\alpha)} / \tilde{p}, \quad (21)$$

similarly,

$$\dot{R}_1 = -u_1(0) = c_m X(0)^{1/(1+\alpha)} / \tilde{p}, \quad (22)$$

where the argument 0 represents values at $r = 0$. From those,

$$f = [X(0)/X_2]^{1/(1+\alpha)}. \quad (23)$$

Thus, the motion of the front is described by

$$\dot{R}_d = \frac{dR}{d\tau} = \dot{R}_1 - f \frac{1}{\tilde{p}} \frac{d-1}{R_d} X_2. \quad (24)$$

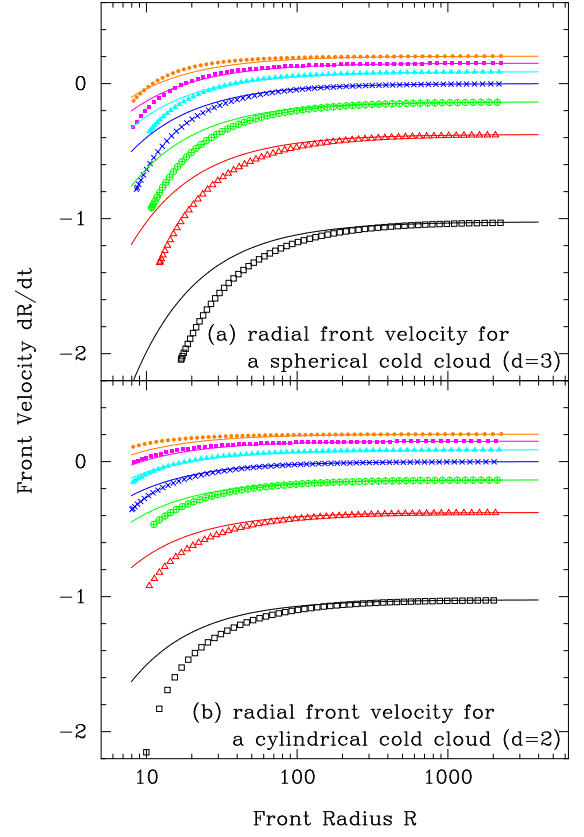


FIG. 2.— The same as Fig.1 but for the front velocity, \dot{R}_d . The curves and symbols represent the approximate solution, eq.(24), and the numerical solution given by eqs.(16) and (17). From the top to the bottom, $\tilde{p} = 1.3, 1.2, 1.1, 1, 0.9, 0.8$ and 0.7 , respectively.

Fig.2 shows the same as Fig.1 but for the front velocity \dot{R}_d . At $R_d \gtrsim 10^2$, the approximate solutions well agree with the numerical ones. On the other hand, At $R_d \lesssim 10^2$, the deviation of the approximate solutions from the numerical ones becomes large. This might suggest that the way of estimating f is too simple because we have found that the fluid velocity itself is well approximated by eq.(20). Nevertheless, eq.(24) well describes the critical radius, $R_{\text{crit},d}$, at which $\dot{R}_d = 0$,

$$R_{\text{crit},d} = \frac{d-1}{c_m} X_2^{\alpha/(1+\alpha)} = -\frac{d-1}{\tilde{\rho}u_1} \tilde{T}_2^\alpha, \quad (25)$$

where $T_2 \equiv X_2^{1/(1+\alpha)}$. In fact, we have found that we can obtain a better fit when we replace f by $f/\tilde{p}^{1+\alpha}$, while it makes the good estimation of $R_{\text{crit},d}$ worse.

In the expression of eq.(24), an undesirable dependence on the temperature at the front remains, whose definition also has an ambiguity. This should be removed by replacing X_2 and R in the curvature term by values at the maximum of $X'X$. To do this, however, the thickness of the front should be explicitly considered. This will be done in a subsequent work. Nevertheless, we have found that it provides a good fit to numerically obtained solutions when the front is defined at the unstable equilibrium in the case of the saturation pressure, $\tilde{p} = 1$. Apart from this, we would like to stress that the above approximate solution can be derived from values \dot{R}_1 and f in $d = 1$ case.

Finally, we discuss the dependence of the front velocity on the front position. As mentioned in §1, Shaviv & Regev

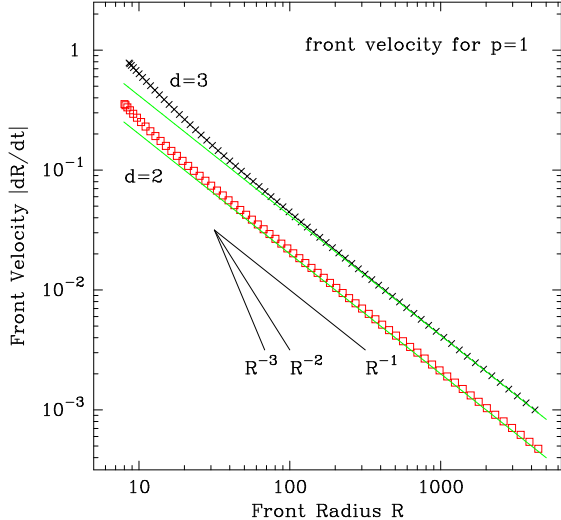


FIG. 3.— The absolute value of the front velocity $|\dot{R}|$ against R . To see its radial dependence, the vertical axis is logarithmic. The straight lines and symbols represent the front velocity provided by the approximate solution and the numerical solution, respectively. The upper and lower sets indicate $d = 3$ and 2, respectively. It is evident that our results are proportional to R^{-1} different from the prediction by Shaviv & Regev (1994).

(1994) considered the frontal motion based on a model equation similar to the TDGL equation. They found that $\dot{R} \propto R^{-d}$ when pressure is nearly equal to the saturation pressure, and $\dot{R} \propto R^{-(d-1)}$ when far from the saturation pressure. Because we have already shown in Fig.2 that $\dot{R} \rightarrow \text{const.}$ as $R \rightarrow \infty$ when far from the saturation pressure, we show the case of $\tilde{p} = 1$, in which we can see only the curvature effects. Fig.3 shows a log-log plot for $|\dot{R}_d|$ against R for $d = 2$ and 3. It is evident that the front velocity is proportional to R^{-1} independent of d . Thus we conclude that the TDGL equation provided in the Lagrangian coordinate does not provide a correct model for thermally bistable fluids.

4. GENERAL CURVED FRONTS

Using the curvature term derived in the previous section, we discuss the dynamics of general curved fronts according to Bray (1994). We take a unit vector normal to the front, \hat{g} , with a direction from the CNM to the WNM. Using this, we can write $\nabla X = (\partial_g X)_\tau \hat{g}$ and $\nabla^2 X = (\partial_g^2 X)_\tau + (\partial_g X)_\tau \nabla \cdot \hat{g}$. Substituting these into equation (19), we obtain

$$u_d (\partial_g X)_\tau = \left[(\partial_g^2 X)_\tau + (\partial_g X)_\tau \nabla \cdot \hat{g} \right] \frac{X}{\tilde{p}} + \frac{1+\alpha}{\alpha} X^{1/(1+\alpha)} F[Z], \quad (26)$$

As done in the previous section, substituting corresponding terms in the right hand side with the one-dimensional equation and noting the existence of the direction cosine against the normal direction in the case of a straight front, we obtain

$$V_d = \cos \theta [\dot{R}_1 - f X_2 K / \tilde{p}], \quad (27)$$

where V_d is the velocity of the front against the normal direction in the case of a straight front, and $K = \nabla \cdot \hat{g}$ is the mean curvature. When we take R_d as a curvature radius, we obtain

$K = (d-1)/R_d$. This result is applicable to general curved fronts.

Let us consider a convex region of the CNM against the WNM, in which $K > 0$. When the CNM is evaporating ($\tilde{p} < 1$), the sign of \dot{R}_1 is negative. Because the sign of the second term is always negative, the CNM in the convex region evaporates faster than in concave regions. When the CNM is accreting cooling WNM ($\tilde{p} > 1$), the sign of \dot{R}_1 is positive. Thus the condensation in the convex region is slower than in concave regions. Consequently, the curvature term always smooths out the curved front. Note that this conclusion is valid only under the assumptions that flows are normal to the front and that the structure of the front is the same as that in the case of plane-parallel geometry.

5. CONCLUSIONS AND DISCUSSION

We have investigated the dynamics of thermally bistable fluids from a pattern-theoretical point of view. To evaluate the curvature effects of the front connecting the WNM and CNM, at first, we focused on d -dimensional spherically symmetric CNM clouds. Using a way of approximations often used in the field of pattern formation theories, we derived an approximate solution describing the velocity of the front. Comparing with numerical solutions, we confirmed that they are in good agreement with each other, at least when the cloud size is larger than a few tens times the Field length, which corresponds to the thickness of the front. We have also found that our results contradict those given by Shaviv & Regev (1994), which assumed a model equation similar to the TDGL equation. We showed that the velocity of the front is proportional to the inverse of the radius in the case of the saturation pressure, and is constant in the case of much larger clouds and/or pressure far from the saturation pressure. Second, we discussed the dynamics of general curved fronts. Using the obtained approximate solution, we have found that the curvature effects smooth out curved fronts.

The latter conclusion apparently contradicts recent numerical experiments of interstellar turbulence (Koyama & Inutsuka 2002, 2005), in which most fronts are unstable. This contradiction might come from our simple assumptions that the structure of the front is independent of geometry and that the fluid motion is normal to the front. Presumably some instability mechanisms are there similar to the Darrieus-Landau instability in propagating flame (Landau & Lifshitz 1987; Inoue & Inutsuka 2005), or the Mullins-Sekerka instability in crystal growth (Mullins & Sekerka 1963, 1964). We are planning to analyze the stability of the front considering these known mechanisms, as well as the validity of the isobaric evolution. Together with those, hydrodynamic simulations will be performed to be compared with the results obtained in this paper.

ACKNOWLEDGMENTS

We would like to thank Tsuyoshi Inoue for useful discussion. MN is supported by the Japan Society for the Promotion of Science for Young Scientists (No.207). MN also thank Yasuhiro Hieida for inviting me to the world of non-equilibrium statistical physics.

REFERENCES

Bray, A. J. 1994, *Advances in Physics*, 43, 357

Cowie, L. L., & McKee, C. F. 1977, *ApJ*, 211, 135

Elphick, C., Regev, O., & Spiegel, E. A. 1991, *MNRAS*, 250, 617

Elphick, C., Regev, O., & Shaviv, N. 1992, *ApJ*, 392, 106 (ERS92)

Field, G. B. 1965, *ApJ*, 142, 531

Ferrara, A., & Shchekinov, Yu. 1993, *ApJ*, 417, 595

Field, G. B., Goldsmith, D. W., & Habing, H. J. 1969, *ApJ*, 155, L149

Graham, R., & Langer, W. D. 1973, *ApJ*, 179, 469

Hennebelle, P., & Pérault, M. 1999, *A&A*, 351, 309

Inoue, T., & Inutsuka, S. in preparation

Koyama, H., & Inutsuka, S. 2002, *ApJ*, 564, L97

Koyama, H., & Inutsuka, S. 2004, *ApJ*, 602, L25

Koyama, H., & Inutsuka, S., in preparation

Kritsuk, A. G., & Norman, M. L. 2002a, *ApJ*, 569, L127

Kritsuk, A. G., & Norman, M. L. 2002b, *ApJ*, 580, L51

Landau, L. D., & Lifshitz, E. 1987, *Fluid Mechanics* (New York: Pergamon)

McKee, C. F., & Begelman, M. C. 1990, *ApJ*, 358, 392

McKee, C. F., & Ostriker, J. P. 1977, *ApJ*, 218, 148

Mullins, W. W., & Sekerka, R. F. 1963, *J. Appl. Phys.*, 34, 323

Mullins, W. W., & Sekerka, R. F. 1964, *J. Appl. Phys.*, 35, 444

Penston, M. V., & Brown, F. E. 1970, *MNRAS*, 150, 373

Shaviv, N. J., & Regev, O. 1994, *Phys. Rev. E*, 50, 2048

Wolfire, M. G., McKee, C. F., Hollenbach, D., & Tielens, A. G. G. M. 2003, *ApJ*, 587, 278

Zel'dovich, Ya. B., & Pikel'ner, S. B. 1969, *JETP*, 29, 170